

Propagation failure of traveling waves in a discrete bistable medium

Gábor Fátth^a

*Institute of Theoretical Physics, University of Lausanne,
CH-1015 Lausanne, Switzerland*

(July 22, 2018)

Propagation failure (pinning) of traveling waves is studied in a discrete scalar reaction-diffusion equation with a piecewise linear, bistable reaction function. The critical points of the pinning transition, and the wavefront profile at the onset of propagation are calculated exactly. The scaling of the wave speed near the transition, and the leading corrections to the front shape are also determined. We find that the speed vanishes logarithmically close to the critical point, thus the model belongs to a different universality class than the standard Nagumo model, defined with a smooth, polynomial reaction function.

I. INTRODUCTION

Reaction-diffusion equations possessing traveling wave solutions have wide applications in various fields, from chemistry and biology to physics and engineering.¹ Even though the underlying physical systems are often composed of discrete elements, such as biological cells, the continuum approximation, described by partial differential equations, usually works well for realistic model parameters. However, there are important exceptions when the intrinsic discrete character of the medium manifests itself, and the resulting phenomena cannot be adequately described without incorporating the discreteness into the mathematical model.

A typical example, when spatial discreteness plays a crucial role, is the phenomenon of *propagation failure* or *pinning* of traveling waves. Consider the scalar reaction-diffusion equation (Nagumo equation)

$$\frac{\partial u}{\partial t} = D \frac{\partial^2 u}{\partial x^2} + f(u), \quad (1)$$

where $u = u(x, t)$ is the chemical concentration function, and D is the diffusion constant. The reaction function $f(u)$ is assumed to be bistable (Nagumo-type), and depends on a parameter a , $0 < a < 1$, such that

$$f(0) = f(a) = f(1) = 0,$$

and

$$\begin{aligned} f(u) < 0 & \quad \text{if } 0 < u < a, \\ f(u) > 0 & \quad \text{if } a < u < 1. \end{aligned}$$

It is known² that whenever $\int_0^1 f(u) du \neq 0$, Eq. (1) possesses a unique, stable traveling wave solution of the form

$$u(x, t) = U(z), \quad z = x - ct, \quad (2)$$

for any value of D . The diffusion constant, which can be scaled to unity by rescaling x , only influences the wave speed c in a trivial manner

$$c = c_0 D^{1/2}, \quad (3)$$

where c_0 is independent of D .

The *discrete* analog of Eq. (1) is defined as

$$\frac{\partial u_n}{\partial t} = D(u_{n-1} + u_{n+1} - 2u_n) + f(u_n). \quad (4)$$

Now the concentration function u_n takes values only on a one-dimensional lattice $n \in Z$. In contrast to the continuum case, traveling wave solutions only exist if the coupling between the lattice sites is strong enough. For weak diffusion, propagation is impeded and, instead, a series of stable steady state solutions emerge. The critical value D_c where the pinning transition occurs depends on the actual reaction function $f(u)$ and is not universal. However, it is believed that the type of the transition, i.e., the way c tends to zero as $D \rightarrow D_c^+$ (from above) is universal, and only depends on some global properties of $f(u)$.

The phenomenon of propagation failure in bistable systems have been intensively studied in the last decade by several authors: Keener³ studied propagation failure in the discrete Nagumo equation and in some of its generalizations, like the FitzHugh-Nagumo or the Beeler-Reuter models, in the context of stimulus conduction in the myocardial tissue. He demonstrated that for weak coupling no propagation is possible, and found lower and upper bounds for the critical coupling $D_c = D_c(a)$ as a function of the reaction function parameter a . He also showed using perturbation theory that in the large D limit the leading correction to the wave speed is an effective shift in D so that

$$c = c_0(D - K)^{1/2}, \quad (5)$$

where the constant K can be obtained by quadrature from the (known) solution of the associated continuum problem in Eq. (1).

A rigorous proof that for strong enough coupling D Eq. (4) indeed has stable traveling wave solutions in the form of Eq. (2), with x replaced by n , was later given by Zinner.⁴

More recently, Erneux and Nicolis⁵ suggested a general theory for the critical behavior near the pinning transition. Using series expansion techniques and bifurcation theory arguments they concluded that as the transition

point is approached c must vanish according to a power law

$$c \sim (D - D_c)^{1/2}, \quad D \rightarrow D_c^+ \quad (6)$$

for $f(u)$ fixed. Of course, despite the formal similarity of Eqs. (5) and (6), the transition point D_c cannot be identified with the constant K of Eq. (5), even though their numerical values may be close.⁶

The above theory of wave propagation and its failure in discrete media has also been fruitfully applied to understand experimental observations in linear arrays of continuously stirred tank reactors,⁷ coupled Chua circuits,^{6,8} and in the theory of excitable cables.⁹ Applications to morphogenetic pattern formation and cellular differentiation are also under investigation.¹⁰

In this paper we analyze the phenomenon of propagation failure for the piecewise linear reaction function

$$f(u) = \begin{cases} -u & \text{if } u \leq a \\ 1 - u & \text{if } u > a. \end{cases} \quad (7)$$

This is a case when the a -dependence of the critical coupling D_c can be analytically found and the pinning transition can be directly studied by relatively simple mathematical tools. Our principal aim is to investigate the critical behavior of the system around D_c , and derive the scaling law of the wave speed. At the same time, we obtain the leading corrections to the wavefront profile $U(z)$.

The organization of the paper is as follows: Section II gives an overview of the traveling wave solutions in the continuum case. Section III treats the discrete model, and consists of five subsections discussing (A) the steady state solutions, (B) their stability, (C) the front shape at the transition point, (D) the leading corrections to the front shape for slow waves, and (E) the scaling law of the speed close to the transition point. Finally, Sec. IV summarizes and discusses the main results.

II. CONTINUOUS MODEL

In this section we look for traveling wave solutions of Eq. (1) defined with the reaction function Eq. (7). Substituting the form of Eq. (2) into Eq. (1), we obtain the ordinary differential equation

$$DU'' + cU' + f(U) = 0. \quad (8)$$

We impose the boundary conditions

$$U(-\infty) = 1 \quad U(\infty) = 0 \quad U(0) = a, \quad (9)$$

and suppose that the wavefront $U(z)$ is monotonically decreasing. Thus Eq. (8) can be written as

$$DU'' + cU' - U + \Theta(-z) = 0, \quad (10)$$

where $\Theta(z)$ is the conventional step function. To solve this equation we use the Fourier transform technique,

which allows a direct generalization to the discrete case later in Sec. III C.

Introducing the Fourier transform

$$V(k) = \mathcal{F}[U(z)] = \int_{-\infty}^{\infty} U(z)e^{ikz} dz \quad (11)$$

Eq. (10) transforms into

$$-k^2 DV(k) - ickV(k) - V(k) - \frac{i}{k} + \pi\delta(k) = 0.$$

This can be solved for $V(k)$ yielding

$$V(k) = V_1(k) + V_2(k),$$

with

$$V_1(k) = \frac{-i}{k(ick + Dk^2 + 1)},$$

$$V_2(k) = \frac{\pi\delta(k)}{ick + Dk^2 + 1}. \quad (12)$$

Note that $V_1(k)$ in Eq. (12) has three simple poles at $k = 0, i\kappa_+, i\kappa_-$ with

$$\kappa_{\pm} = \frac{1}{2D} \left(-c \pm \sqrt{c^2 + 4D} \right), \quad (13)$$

thus the inverse transformation is straightforward. We obtain

$$\mathcal{F}^{-1}[V_1(k)] = \frac{1}{2} - \Theta(z) - \frac{e^{\kappa_+ z} \Theta(-z)}{D\kappa_+(\kappa_+ - \kappa_-)} - \frac{e^{\kappa_- z} \Theta(z)}{D\kappa_-(\kappa_+ - \kappa_-)}, \quad (14)$$

$$\mathcal{F}^{-1}[V_2(k)] = \frac{1}{2}, \quad (15)$$

which leads to

$$U(z) = -\frac{e^{\kappa_+ z} \Theta(-z)}{D\kappa_+(\kappa_+ - \kappa_-)} - \frac{e^{\kappa_- z} \Theta(z)}{D\kappa_-(\kappa_+ - \kappa_-)} + \Theta(-z). \quad (16)$$

The continuity of $U(z)$ and its derivative at the origin is automatically satisfied by this expression, irrespective of the value of c . The second derivative, however, has a jump discontinuity at $z = 0$.

The wave speed can be obtained from the requirement $U(0) = a$ in Eq. (9). This gives the constraint

$$\frac{-1}{D\kappa_-(\kappa_+ - \kappa_-)} = a,$$

from which c turns out to be

$$c = (1 - 2a) \sqrt{\frac{D}{a(1-a)}}. \quad (17)$$

Note that this expression indeed satisfies the general form Eq. (3). We find that the speed changes sign at $a = 1/2$,

and around this value it behaves linearly. Furthermore, c diverges whenever $a \rightarrow 0$ or 1. Using Eq. (17), the wave front profile in Eq. (16) reduces to

$$U(z) = \begin{cases} 1 - (1-a)e^{\kappa_+ z} & \text{if } z \leq 0 \\ ae^{\kappa_- z} & \text{if } z \geq 0, \end{cases} \quad (18)$$

where κ_{\pm} is

$$\kappa_+ = \sqrt{\frac{a}{(1-a)D}}, \quad \kappa_- = -\sqrt{\frac{1-a}{aD}}.$$

The wave front profile for $a = 0.2$, and the a -dependence of the speed for the continuum model is shown in Fig. 1.

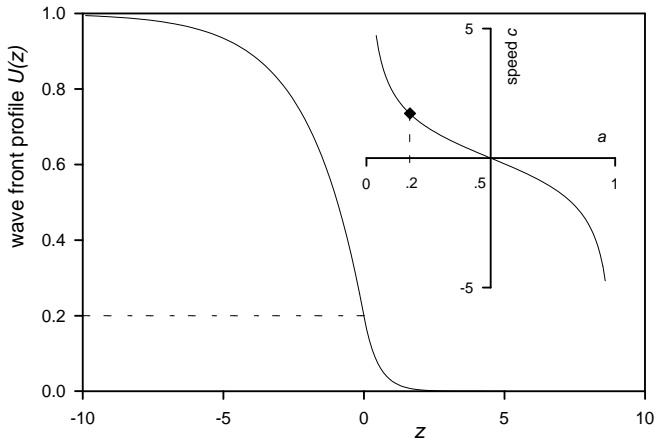


FIG. 1. Wave front profile $U(z)$ in the continuum case for the diffusion constant $D = 1$ and the reaction function parameter $a = 0.2$. The associated wave speed is $c = 1.5$. The inset shows the wave speed for general a .

III. DISCRETE MODEL

We now turn to the analysis of the discrete problem defined by Eq. (4) and (7).

A. Steady states and virtual steady states

The critical curves of the pinning transition on the (D, a) parameter plane can be obtained by analyzing the range of existence of monotonic steady state solutions.³ We investigate under what conditions a monotonically decreasing steady state can exist with the boundary conditions $u_{-\infty} = 1$, $u_{\infty} = 0$. Clearly, if such a solution exists, due to translational invariance, an infinite series of solutions can be constructed. In the following, any distribution u_n^M of the concentration values that satisfies the inequalities

$$\begin{aligned} u_n^M &> a \quad \text{if } n < M \\ u_n^M &\leq a \quad \text{if } n \geq M, \end{aligned} \quad (19)$$

will be referred to as the *kink- M* distribution (solution). We introduce the superscript M to explicitly denote the position of the kink, lying between sites $M - 1$ and M . Such kink distributions contain two different domains. The sites on the left (right) side of the kink are subject to the high (low) concentration branch of the piecewise linear $f(u)$ function.

As is shown by Eq. (17), the continuum problem possesses steady state solutions (traveling wave solutions with $c = 0$) for a given D only when $a = 1/2$. In contrast, in the discrete version, monotonic steady state kinks persist over a wide range of values of a . The calculation of this range as a function of D for the piecewise linear reaction function in Eq. (7) is straightforward: Providing that Eq. (19) holds, a candidate kink- M steady state solution $u_n(t) = s_n^M$ can be looked for in the form

$$s_n^M = \begin{cases} 1 - A_+ e^{\kappa n} & \text{if } n < M \\ A_- e^{-\kappa n} & \text{if } n \geq M. \end{cases} \quad (20)$$

Substituting this expression into Eq. (4), the inverse diffusion length κ reads

$$\kappa = \cosh^{-1} \left(\frac{1}{2D} + 1 \right), \quad (21)$$

while the two constants A_+ and A_- turn out to be

$$A_{\pm} = a_{\pm} e^{\mp \kappa M}, \quad (22)$$

with the M -independent part defined by

$$a_{\pm} = \frac{1}{2} \left(1 \pm \frac{1}{\sqrt{1 + 4D}} \right). \quad (23)$$

Note, however, that s_n^M in Eq. (20) is a valid kink- M steady state only if it satisfies the inequalities in Eq. (19). Since s_n^M is monotonically decreasing, the conditions $s_{M-1}^M > a$ and $s_M^M \leq a$ are necessary and sufficient. From Eq. (20) we find that

$$s_{M-1}^M = a_+, \quad s_M^M = a_-,$$

thus we conclude that monotonically decreasing steady states exist for a given D only if $a_- < a < a_+$, where $a_{\pm} = a_{\pm}(D)$ is expressed by Eq. (23). We point out that the shape of the steady state, when it exists, do not depend on the actual parameter a , but only on the diffusion constant D .

The values of $a_- = a_-(D)$ and $a_+ = a_+(D)$ are plotted in Fig. 2 as a function of the diffusion constant D . As was argued by Keener³, the existence of steady state solutions impede propagation, thus traveling wave solutions do not exist in the shaded region (pinning region) of the figure. They do exist, however, when the parameter pair (D, a) lies outside the shaded regime, i.e., if $a < a_-$ or $a > a_+$. In such cases, the concentration distribution s_n^M defined by Eqs. (20–22) is not a valid steady state. Thus, because of the role it plays in the description of the dynamics of traveling waves, we will refer to it in later sections as the *virtual kink- M* steady state.

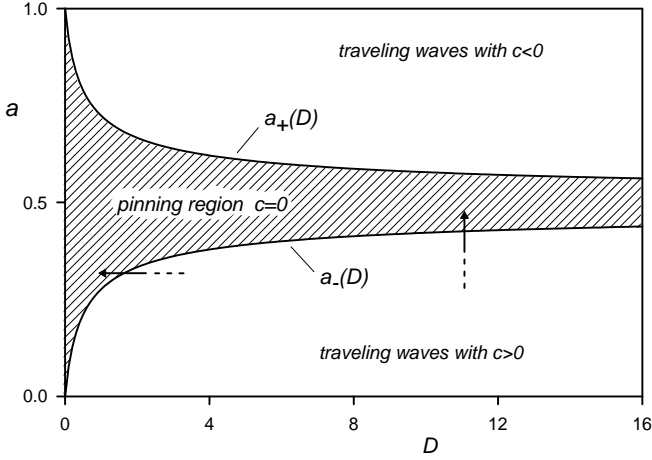


FIG. 2. Phase diagram on the a vs D plane. Pinned steady state solutions exist in the shaded region, while traveling waves exist in the unshaded ones. The pinning transition takes place along the $a = a_+(D)$ and the $a = a_-(D)$ curves, and can be initiated either by changing D for a fixed, or by varying a with D fixed (see arrows).

B. Stability of the kink- M steady state

To assess the stability of the kink- M steady state, we introduce a perturbation $\delta u_n(t)$ as

$$u_n(t) = s_n^M - \delta u_n(t). \quad (24)$$

Substituting Eq. (24) into Eq. (4), the dynamics of the perturbation is found to satisfy the equation

$$\frac{\partial \delta u_n}{\partial t} = D(\delta u_{n-1} + \delta u_{n+1} - 2\delta u_n) - \delta u_n. \quad (25)$$

This is the discrete diffusion equation with an additional spatially uniform decay term. Clearly, it only has decaying solutions, so our kink- M steady state is *stable*.

Nevertheless, for use in later sections, we investigate Eq. (25) further. Introducing the Fourier transform and the Laplace transform of $\delta u_n(t)$ as

$$\begin{aligned} \delta u(k, t) &= \sum_{n=-\infty}^{\infty} \delta u_n(t) e^{ikn}, \\ \delta u_n(s) &= \int_0^{\infty} dt \delta u_n(t) e^{-st}, \end{aligned}$$

respectively, we find

$$\delta u(k, s) = \frac{\widetilde{\delta u}(k, 0)}{s + 2D(1 - \cos k) + 1},$$

where $\widetilde{\delta u}(k, 0)$ is the Fourier transform of the initial perturbation at time $t = 0$. Inverting the transformations we obtain

$$\delta u_n(t) = \int_{-\pi}^{\pi} \frac{dk}{2\pi} \widetilde{\delta u}(k, 0) e^{-[1+2D(1-\cos k)]t} e^{-ikn}.$$

The fundamental solution (Green's function) of Eq. (25), i.e., the dynamics for the initial condition $\delta u_n(0) = \delta_{n,m}$ turns out to be

$$\delta u_n(t) = e^{-(1+2D)t} \int_{-\pi}^{\pi} \frac{dk}{2\pi} e^{2Dt \cos k} \cos[k(n-m)].$$

Noting that the definition of the modified Bessel function of integer order $I_n(z)$ is¹¹

$$I_n(z) = \frac{1}{\pi} \int_0^{\pi} e^{z \cos \theta} \cos(n\theta) d\theta,$$

we can write the fundamental solution as

$$\delta u_n(t) = e^{-(1+2D)t} I_{n-m}(2Dt). \quad (26)$$

C. Front shape at $c = 0^+$

The Fourier transform method can be used to determine the shape of the propagating front $U_0(z)$ in the limit $c \rightarrow 0^+$. Introducing $z = n - ct$, we look for solutions in the form

$$u_n(t) = U(z).$$

The wave front profile function $U(z)$ satisfies the functional differential equation

$$D[U(z-1) + U(z+1) - 2U(z)] + \quad (27)$$

$$cU'(z) - U(z) + \Theta[U(z) - a] = 0, \quad (28)$$

containing “advanced” and “delayed” terms of the continuous variable z . Supposing that $U(0) = a$ and $U(z)$ is monotonically decreasing, the last term can be rewritten as

$$\Theta[U(z) - a] = \Theta(-z).$$

Fourier transforming, using the definition in Eq. (11), yields

$$2D(\cos k - 1)V(k) - ickV(k) - V(k) - \frac{i}{k} + \pi\delta(k) = 0, \quad (29)$$

which can be solved for $V(k)$ as

$$V(k) = V_1(k) + V_2(k),$$

with

$$\begin{aligned} V_1(k) &= \frac{-i}{k[ikc + 2D(1 - \cos k) + 1]}, \\ V_2(k) &= \frac{\pi\delta(k)}{ikc + 2D(1 - \cos k) + 1}. \end{aligned} \quad (30)$$

These expressions only differ from those in Eq. (12) in that they contain $2(1 - \cos k)$ instead of k^2 .

As before, $V_2(k)$ only contributes as a uniform shift of $1/2$ to $U(z)$. The inverse Fourier transform of the $V_1(k)$ term is more subtle, since now it has an infinite series of poles due to the different branches of the $\cos k$ function. Explicit form of $U(z)$ can only be obtained in the limit $c = 0^+$.

When $c = 0$, we use Eq. (21) to write $V_1(k)$ as

$$V_1(k) = \frac{i}{\sqrt{4D+1}} \frac{1}{k} \left[\frac{1}{1 - e^{ik+\kappa}} + \frac{1}{1 - e^{ik-\kappa}} \right].$$

After some trivial manipulations to assure convergence, the two terms can be rewritten as infinite sums of geometrical series, leading to

$$\begin{aligned} V_1(k) &= \frac{-i}{\sqrt{4D+1}} \frac{1}{k} \left[\sum_{n=1}^{\infty} e^{-ikn} e^{-\kappa n} + \sum_{n=0}^{\infty} e^{ikn} e^{-\kappa n} \right] \\ &= \frac{-i}{\sqrt{4D+1}} \frac{1}{k} \left[1 + 2 \sum_{n=1}^{\infty} \cos(kn) e^{-\kappa n} \right]. \end{aligned}$$

According to mathematical handbooks,¹²

$$\begin{aligned} \mathcal{F}^{-1} \left[\frac{-i}{k} \right] &= -\frac{1}{2} + \Theta(-z), \\ \mathcal{F}^{-1} \left[\frac{-2i}{k} \cos(kn) \right] &= \Theta(-n-z) - \Theta(z-n), \end{aligned}$$

thus, collecting all the terms, the final result for $U_0(z) \equiv \lim_{c \rightarrow 0^+} U(z)$ is

$$U_0(z) = a_- + \frac{1}{\sqrt{4D+1}} \left\{ \Theta(-z) + \sum_{n=1}^{\infty} [\Theta(-n-z) - \Theta(z-n)] e^{-\kappa n} \right\}.$$

This function is plotted in Fig. 3 as curve (a).

As is seen, $U_0(z)$ contains a series of plateaus separated by jump discontinuities. Consequently, the propagation of the front in the $c \rightarrow 0^+$ limit is characterized by an (infinitely) long *waiting* period, when the concentrations hardly change, followed by a rapid *jump* period, when the front steps ahead a lattice site. We can calculate the values of $U_0(z)$ on the plateaus, i.e., in the waiting period. We obtain that for any z in the range $n < z < n+1$

$$U_0(z) = \begin{cases} 1 - a_+ e^{\kappa n} & \text{if } n < 0 \\ a_- e^{-\kappa n} & \text{if } n \geq 0. \end{cases}$$

Comparing this formula to Eq. (20), we see that the plateau values coincide with the concentration values in the a -independent steady state solution s_n^0 for the given value of D . Thus close to the pinning transition, traveling waves in their waiting period look almost identical to the associated steady states belonging to the same D but to a different a parameter $a_- < a < a_+$.

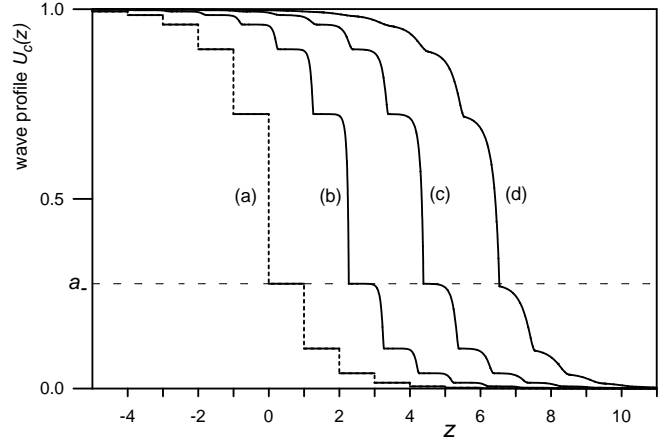


FIG. 3. Wave front profiles $U_c(z)$ near the pinning transition for $D = 1$. The corresponding exact critical point is $a_- = 1/2 - 1/2\sqrt{5} = 0.27639320 \dots$. The four curves belong to different parameters a and velocities c : (a) $a = a_-$, $c = 0$, (b) $a = 0.276393$, $c = 0.0780$, (c) $a = 0.276$, $c = 0.1782$, (d) $a = 0.27$, $c = 0.3246$. Curves (b)–(d) are shifted for better visibility.

D. Leading correction to the front shape

Our next aim is to calculate the leading correction to the shape of the front when $0 < c \ll 1$. When the front propagates with a nonzero speed, the corresponding wavefront profile $U_c(z)$ changes drastically in the narrow *transition layers* around the jump discontinuities of $U_0(z)$, so that $U_c(z)$ becomes *continuous*. While the spacing of these layers is unity (the lattice constant was set to unity), their widths are proportional to c . In the limit $c \rightarrow 0^+$, all the transition layers shrink to instantaneous jumps (see Fig. 3).

Note that the small extra term $cU'(z)$ in Eq. (28) is a *singular perturbation*. When it is absent, i.e., $c = 0$, the order of our functional differential equation Eq. (28) is reduced. The effect of this term on the solution cannot be calculated by regular perturbation theory, i.e., series expansion with respect to the small parameter c . There are regions of the solution function, the transition layers, where $U_c(z)$ deviates in an essentially nonperturbative way from the solution of the unperturbed problem $U_0(z)$. The singular nature of the problem also manifests itself in the Fourier transform $V_1(k)$ in Eq. (30). Since the poles are solutions of a transcendental equation, even the slightest change in the term ikc will substantially modify the pole structure far from the origin.

In order to obtain the functional form in the transition layers, we return to Eq. (4), and analyze its real time dynamics in a small time period directly after the concentration at a given site, say at site 0, has exceeded the value of a . At this moment ($t = 0$) the concentration values in the moving front are distributed in a way that they satisfy the inequalities in Eq. (19) with $M = 1$, i.e.,

the kink is located between sites 0 and 1. We have seen in Sec. III A and B that for such a situation a stable steady state solution exists, namely s_n^1 defined by Eq. (20). Therefore in these very first moments the dynamics of $u_n(t)$ is identical to the gradual approach towards the stable-looking distribution s_n^1 . However, since (D, a) lies outside the pinning region, s_n^1 is only a *virtual* steady state. The dynamical system will never attain such a virtual attractor, because when the system approaches it too closely, the value of $u_1(t)$ exceeds a and the consistency condition Eq. (19) breaks down. At that moment ($t = T$) a new virtual steady state emerges one lattice site ahead, and the whole story repeats itself; this time, from shifted initial conditions. The role of the virtual attractors in the dynamics is schematically illustrated in Fig. 4.

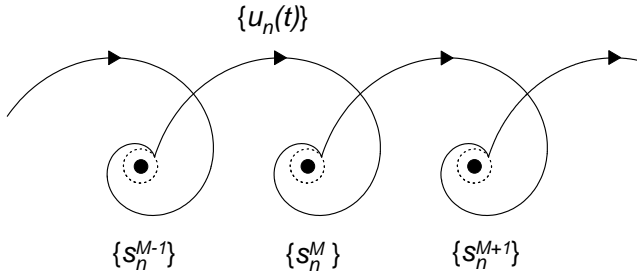


FIG. 4. Schematic illustration of the role of virtual steady states $\{s_n^M\}$ in the dynamics. The continuous curve represents the time evolution of the system in the infinite dimensional vector space $\{u_n\}$. When a virtual attractor (black dot) is approached as close as the dotted circle, the consistency condition breaks down and a new stable-looking attractor emerges one lattice site ahead.

To describe quantitatively the dynamics for $0 < t < T$, we require the initial distribution $u_n(0)$ at $t = 0$. Supposing that the front propagates very slowly, $c \equiv 1/T \ll 1$, we can use the observation that the transition layers are very narrow. Consequently, $u_n(0)$ is well approximated by $u_n(0) \approx s_n^0$. Defining the deviation function $\delta u_n(t) > 0$ by

$$u_n(t) = s_n^1 - \delta u_n(t),$$

we conclude that in the time interval $0 < t < T$ the dynamics of $\delta u_n(t)$ is given exactly by Eq. (25) with the approximate initial condition at $t = 0$

$$\delta u_n(0) = s_n^1 - s_n^0 = \frac{1}{\sqrt{1+4D}} e^{-\kappa|n|}.$$

Using the fundamental solution in Eq. (26), $\delta u_n(t)$ can be expressed as

$$\delta u_n(t) = \frac{e^{-(1+2D)t}}{\sqrt{1+4D}} \Sigma_n(2Dt), \quad (31)$$

where $\Sigma_n(\tau)$ is defined as an infinite sum involving Bessel functions

$$\Sigma_n(\tau) \equiv \sum_{m=-\infty}^{\infty} e^{-\kappa|m|} I_{n-m}(\tau).$$

Unfortunately, $\Sigma_n(\tau)$ cannot be expressed in a closed form with known functions, but it can be reduced to quadrature: Introducing the function

$$F(c, \tau) \equiv \sum_{m=0}^{\infty} c^m I_m(\tau),$$

and its integral representation¹³

$$F(c, \tau) = \exp\left(\left[c + \frac{1}{c}\right] \frac{\tau}{2}\right) - \frac{1}{c\tau} \exp\left(\frac{\tau}{2c}\right) \int_0^\tau d\xi \xi \exp\left(\frac{-\xi^2}{2\tau c}\right) I_0(\xi),$$

we obtain

$$\Sigma_n(\tau) = 2 \cosh(\kappa n) F(e^{-\kappa}, \tau) - e^{\kappa n} I_0(\tau) - 2 \sum_{m=1}^{n-1} \sinh[\kappa(n-m)] I_m(\tau). \quad (32)$$

This expression only contains a finite sum of $n-1$ terms involving Bessel functions. For large values of n it can also be expressed in an even more compact form using another special integral, but we will not need that form here. Figure 5 shows the deviation function $\delta u_n(t)$, calculated from Eqs. (31) and (32), for some small values of n .

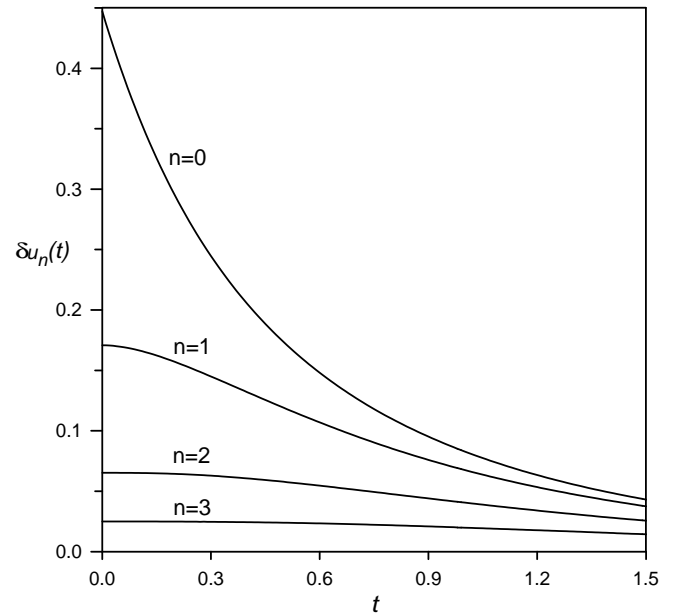


FIG. 5. The deviation function $\delta u_n(t)$ is plotted vs t for $n = 0, 1, 2$ and 3 . Except the $n = 0$ curve, all the curves start with zero slope at $t = 0$.

Having solved the dynamics for $\delta u_n(t)$ in Eq. (31), we are ready to express the leading correction to the wave front profile in the slow propagation limit. Using the formal definition $\delta u_n(t) = 0$ for $t < 0$, we write the continuous function $U_c(z)$ in the compact form

$$U_c(z) = U_0(z) - \sum_{n=-\infty}^{\infty} \delta u_n \left(\frac{n-z}{c} \right), \quad (33)$$

recalling that for each n the correction term $\delta u_n[(z-n)/c]$ is negligibly small everywhere, except in the narrow layer $n - \mathcal{O}(c) < z < n$.

There are two limits in which the functional form of $\delta u_n(t)$, and hence that of $U_c(z)$ simplifies. For small τ , the $F(c, \tau)$ function can be expanded as

$$F(c, \tau) \simeq 1 + \frac{c}{2}\tau + \frac{c^2 + 2}{8}\tau^2 + \mathcal{O}(\tau^3).$$

Using this and the standard small argument expansions of the Bessel functions, we obtain from Eq. (32)

$$\Sigma_n(\tau) \simeq \begin{cases} 1 + e^{-\kappa} \tau + \mathcal{O}(\tau^2) & \text{if } n = 0 \\ e^{-n\kappa} [1 + \cosh(\kappa) \tau + \mathcal{O}(\tau^2)] & \text{if } |n| \geq 1. \end{cases}$$

Hence, using Eq. (21), we find that for $n = 0$

$$\delta u_0(t) \simeq \frac{1}{\sqrt{1+4D}} - t + \mathcal{O}(t^2),$$

and for $|n| \geq 1$

$$\delta u_n(t) \simeq \frac{e^{-\kappa n}}{\sqrt{1+4D}} + \mathcal{O}(t^2).$$

It is seen that only $\delta u_0(t)$ starts with a finite slope at $t = 0$, while for all $|n| \geq 1$ the slope of $\delta u_n(t)$ is zero (see Fig. 5). Consequently, the jump discontinuities of $U_0(z)$ round off everywhere; $U_c(z)$ becomes continuous and differentiable for all z , except at the origin, defined by $U_c(0) = a$, where the function retains a cusp (see Fig. 3).

E. Speed scaling near the transition point

The other limit that we investigate is the large t limit. Using the large argument expansion of the Bessel functions¹¹

$$I_m(\tau) \simeq \frac{e^\tau}{\sqrt{2\pi\tau}} \left[1 + \mathcal{O}\left(\frac{m^2}{\tau}\right) \right],$$

we can directly evaluate $\Sigma_n(\tau)$ in leading order as

$$\Sigma_n(\tau) \simeq \frac{e^\tau}{\sqrt{2\pi\tau}} \sum_{m=-\infty}^{\infty} e^{-\kappa|m|} = \frac{e^\tau}{\sqrt{2\pi\tau}} \coth \frac{\kappa}{2}.$$

Substituting this formula into Eq. (31), we obtain for large t

$$\delta u_n(t) \simeq \frac{e^{-t}}{\sqrt{4\pi Dt}} + \mathcal{O}\left(\frac{e^{-t}}{t^{3/2}}\right). \quad (34)$$

This result can be used to derive a formula for the wave speed close to the pinning transition: As was discussed above, the next step of the wavefront occurs at time T , when the value of $u_1(T)$ reaches (from below) the actual value of a . We introduce the small variable $\delta\theta = \delta\theta(D, a)$ which measures the difference from the critical point, defined by

$$\delta\theta \equiv a_- - a = \frac{1}{2} \left(1 - \frac{1}{\sqrt{1+4D}} \right) - a.$$

Obviously

$$\delta\theta \simeq \begin{cases} -\delta a & \text{for } D \text{ fixed,} \\ (1+4D)^{-3/2} \delta D & \text{for } a \text{ fixed.} \end{cases}$$

Using Eq. (34), we find that in leading order the time T , required for δu_1 to decrease to the value of $\delta\theta$, satisfies the equation

$$\delta\theta = \frac{e^{-T}}{\sqrt{4\pi DT}}. \quad (35)$$

Thus the wave speed $c \equiv 1/T$ is

$$c = \frac{-1}{\ln(\sqrt{4\pi D} \delta\theta)} + \mathcal{O}\left(\frac{\ln(\ln 1/\delta\theta)}{\ln^2 1/\delta\theta}\right), \quad (36)$$

i.e., it behaves *logarithmically* off the critical point.

Even though the asymptotic form in Eq. (36) is valid as $\delta\theta \rightarrow 0$, we note that the log-log correction term is significant for any numerically feasible values of $\delta\theta$. Thus in order to test the scaling we use Eq. (35) instead, and plot the numerically obtained values of

$$R = \frac{c^{1/2} e^{-1/c}}{\sqrt{4\pi D} \delta\theta} \quad (37)$$

as a function of $\delta\theta$ in Fig. 6. As is seen, the numerical values nicely approach the theoretical limit $R = 1$ as $\delta\theta \rightarrow 0$.

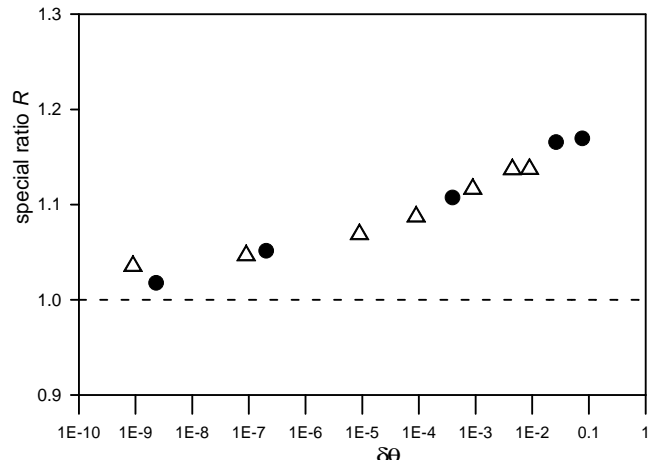


FIG. 6. The special ratio R , defined by Eq. (37), is plotted vs the distance from the critical point $\delta\theta$ for the data obtained by numerical simulation. Circles refer to the case when D is varied, triangles to the one when a is tuned around the critical point $D = 1$, $a = a_-(D) = 1/2 - 1/2\sqrt{5}$. Theoretically R approaches 1 as $\delta\theta \rightarrow 0$.

IV. SUMMARY AND DISCUSSION

In summary, we have studied the phenomenon of propagation failure in a particular discrete bistable reaction-diffusion model, for which the reaction function $f(u)$ is composed of two stable linear branches separated by a jump discontinuity at $u = a$. This model is the simplest caricature of some widely used, more realistic reaction functions such as the smooth polynomial (Nagumo) function

$$f(u) = u(u - a)(1 - u). \quad (38)$$

So far, it was generally believed that the qualitative properties of these models are identical.

In this paper we concentrated on the behavior of the piecewise linear model near the pinning transition. The transition lines were found by identifying the boundaries of the parameter domain (pinning region) where steady state solutions exist. By generalizing the concept of steady states to include virtual steady states, we showed that outside the pinning region the front propagates in a two stage manner: an exponentially rapid “jump-ahead” period is followed by a long “waiting” period when the concentrations hardly change. At each moment the system converges towards one of the stable-looking virtual steady states, which is, however, never reached completely. We derived analytic expressions for the wave front profile $U(z)$ in the slow propagation limit, and argued that it becomes continuously differentiable everywhere except at the origin, defined by $U(0) = a$, where the function retains a cusp singularity.

We also calculated, in leading order, the wave speed as a function of the distance from the critical point. Surprisingly, we found that $c \rightarrow 0$ *logarithmically* as the transition point is approached. This finding is distinct from previous results,⁵ obtained from the analysis of the reaction function in Eq. (38), in which the speed was shown to scale as a *power law* with an exponent $1/2$ in the pinning transition.

It is worth investigating whether the different critical behavior found in our case is only due to the discontinuity of our $f(u)$ function. To see this we analyzed numerically the transition for the case when $f(u)$ is constructed from three linear pieces so that it remains continuous everywhere, but possesses two nonanalytic break points where its derivative jumps,

$$f(u) = \begin{cases} -u & \text{if } u \leq a/2 \\ u - a & \text{if } a/2 \leq u \leq (a + 1)/2 \\ 1 - u & \text{if } u \geq (a + 1)/2. \end{cases} \quad (39)$$

Our results (not shown) indicate that the scaling of the speed near the transition point remains logarithmic in this case, too.

It is clear that the analytic properties of the reaction functions may play an important role in the critical behavior near the pinning transition. It is less evident which singularities, in general, are irrelevant and do not change universality, and which are essential enough to modify the critical behavior, as we found for the ones in Eqs. (7) and (39). The detailed analysis of these questions is left to future investigation.

ACKNOWLEDGMENTS

The author gratefully acknowledges valuable discussions with Z. Domański, P. Erdős and S. B. Haley. This research was supported by the Swiss National Science Foundation Grant No. 20-37642.93.

^a On leave from the Research Institute for Solid State Physics, Budapest, Hungary.

¹ P. C. Fife, *Mathematical Aspects of Reacting and Diffusing Systems*, Lecture Notes in Biomathematics vol. **28**, Springer Verlag, NY, 1979; J. D. Murray: *Mathematical Biology*, Lecture Notes in Biomathematics vol. **19**, Springer Verlag, Berlin, 1989; A. I. Volpert, V. A. Volpert and V. A. Volpert, *Traveling Wave Solutions of Parabolic Systems*, Math. Monograph vol. **140** of the Am. Math. Soc., Providence, 1994; A. C. Scott, *Active and Nonlinear Wave Propagation in Electronics*, Wiley-Interscience, NY, 1970.

² D. G. Aronson and H. F. Weinberger, *Adv. Math.* **30**, 33 (1978); P. C. Fife and J. B. McLeod, *Arch. Rational Mech. Anal.* **65**, 333 (1977).

³ J. P. Keener, *SIAM J. Appl. Math.* **47**, 556 (1987); *J. Theor. Biol.* **148**, 49 (1991).

⁴ B. Zinner, *SIAM J. Math. Anal.* **22**, 1016 (1991); *J. Diff. Eqns.* **96**, 1 (1992).

⁵ T. Erneux and G. Nicolis, *Physica D* **67**, 237 (1993).

⁶ V. Perez-Munuzuri, V. Perez-Villar and L. O. Chua, *Int. J. Bifurcation and Chaos* **2**, 403 (1992).

⁷ J. P. Laplante and T. Erneux, *J. Phys. Chem.* **96**, 4931 (1992).

⁸ T. Sobrino, M. Alonso, V. Perez-Munuzuri and V. Perez-Villar, *Eur. J. Phys.* **14**, 74 (1993); V. Perez-Munuzuri, V. Perez-Villar and L. O. Chua, *J. Circuits, Systems, and Computers* **3**, 215 (1993).

⁹ J. Rinzel, *Ann. NY Acad. Sci.* **591**, 51 (1990).

¹⁰ G. Fáth, unpublished.

¹¹ M. Abramovitz and I. A. Stegun, *Handbook of Mathematical Functions*, US Department of Commerce, 1964.

¹² A. Erdélyi, *Tables of Integral Transforms*, McGraw-Hill, NY, 1954.

¹³ E. R. Hansen, *A Table of Series and Products*, Englewood Cliffs, Prentice-Hall, 1975.